

Extended superscaling with two-particle emission in electron and neutrino scattering

V.L. Martinez-Consentino,^{1,*} J.E. Amaro,^{1,†} P.R. Casale,¹ and I. Ruiz Simo^{1,‡}

¹*Departamento de Física Atómica, Molecular y Nuclear
and Instituto Carlos I de Física Teórica y Computacional
Universidad de Granada, E-18071 Granada, Spain.*

(Dated: July 26, 2023)

An extended superscaling analysis of quasielastic electron scattering data is proposed by parametrizing the scaling function as the sum of a symmetric function corresponding to the emission of a single particle plus a contribution from the phase space of two-particle emission. The phase space of two-particle emission (2p2h) is multiplied by a q -dependent parameter that has been fitted to describe the tail behavior of the scaling function. This approach allows for an alternative description of the quasielastic electron scattering data, incorporating the contributions from both single-particle and two-particle emission processes induced by the one-body current and explaining the asymmetry of the scaling function. In a factorized schematic model based on the independent-pair approximation, the 2p2h parameter is related to the high-momentum distribution of the pair averaged over 2p-2h excitations. However, in the phenomenological fitting approach undertaken here, this coefficient includes other contributions such as interference with two-body currents and effects of the final-state interactions. We present predictions for the inclusive two-nucleon emission cross section induced by electrons and neutrinos.

Keywords: Quasielastic electron scattering, neutrino scattering, Two-particle emission

I. INTRODUCTION

Knowledge of the neutrino-nucleus interaction and the electron-nucleus interaction is essential for current neutrino experiments with accelerators [1–7]. The emission of one nucleon is the most important contribution to the inclusive cross section in the quasi-elastic (QE) region, centered around $\omega = |Q^2|/2m_N^*$, where ω is the energy transfer, $Q^2 = \omega^2 - q^2 < 0$, and q is the momentum transfer to a nucleon with relativistic effective mass m_N^* [8–11]. Recent theoretical work have shown the importance of two-particle (2p2h) excitation in the QE cross section (about 20% of the total cross section) [12–23].

The emission of two particles requires interaction mechanisms with a pair of nucleons. Regardless of the final-state interactions, this can be achieved with meson-exchange currents (MEC) [24, 25] and with short-range correlations (SRC) models [26–29]. Alternatively SRC have also been introduced as a two-body correlation operator [12, 30–33]. In ref. [13] the two-body one-pion exchange operator is modified to include SRC via the Landau Migdal parameters. One effect of SRC is to provide high momentum components to nucleons due to the nuclear force at short distances [28, 29, 34, 35]. This is being exploited to extract the number of SRC pairs from semi-inclusive and inclusive ($e, e'NN$) reactions [36–38]. However, in general, SRC and MEC interfere with each other, and it is not possible to separate or isolate them from other effects such as final-state interactions.

In this work, we present a method to obtain the con-

tribution to the inclusive response of 2p2h (two-particle, two-hole) induced by the one-body current from the phenomenological scaling function. The QE scaling function is obtained from the (e, e') data by dividing by a single nucleon cross section [39–41]. The starting point is the superscaling analysis with relativistic effective mass (SuSAM*) that is based in the relativistic mean field model (RMF) of nuclear matter [8, 9]. The SuSAM* scaling function describes most of the QE events but it contains residual effects due to SRC, MEC and other contributions. In Ref. [22] the MEC 2p2h contribution was subtracted from the (e, e') data, using a RMF calculation, and a new scaling function was obtained without contamination from the MEC 2p2h channel. But this function still contains contributions from other non-QE mechanisms, in particular from 2p2h excitations produced by the one-body current, including SRC, interferences with MEC, and final state interactions (FSI).

To extract the 2p2h contribution of the one-body (OB) current we assume that the tail of the scaling function, $f^*(\psi^*)$, for high values of the scaling variable, ψ^* — or equivalently for high values of the energy transfer — is due mainly to the 2p2h phase space. In particular SRC produce high momentum components in the nuclear wave function while the excitation of nucleons with high momentum implies high values of the scaling variable, $\psi^* > 1$, which gives a contribution to the tail of $f^*(\psi^*)$. It is important to note that the contribution of SRC to the 2p2h response is entangled with other effects, such as interference with MEC and FSI effects. This entanglement makes it not possible to extract the SRC contribution unambiguously from the data alone. In this work we assume that the 2p2h response function induced by OB current can be parametrized with a semiempirical formula similar to that of the MEC responses [23]. By this assumption the 2p2h response will be proportional to

*Electronic address: victormc@ugr.es

†Electronic address: amaro@ugr.es

‡Electronic address: ruizsig@ugr.es

the 2p2h phase space and to the single-nucleon response. The combined effects of SRC, MEC, FSI, and possibly other nuclear dynamics will be encoded in 2p2h parameters fitted to reproduce the tail of the scaling function. Our approach is alternative and complementary to current search on SRC pairs from inclusive electron scattering data in the zone of low energy and high transferred momentum $q > 1.5$ GeV/c. [37].

In this work we focus on intermediate momentum transfer $q \leq 1$ GeV/c. This region is of interest for neutrino experiments where we are going to apply our results. One of the processes we will analyze in this work is the emission of two particles as a result of energy and momentum transfers to a pair of correlated nucleons whose wave function contains high-momentum components. In the independent pair approximation, the high-momentum component is thought to originate from the interaction between nucleon pairs in the nuclear medium, which can be mathematically expressed as the solution to the Bethe-Goldstone (BG) equation. We will demonstrate that the product of the OB current with the high-momentum wave function of a nucleon pair leads to an effective two-body correlation current. If we make the approximation of factorizing an average of the one-body current and the phase space in this model, we obtain a coefficient that is related to the average of the high-momentum distribution of a pair of correlated nucleons.

In our scaling analysis, we observe that the scaled data, when plotted as a function of the scaling variable, exhibit a compatible behavior and can be effectively parameterized as the sum of a symmetric scaling function and a 2p2h-like contribution. This 2p2h-like contribution, proportional to the 2p2h phase space, accurately reproduces the tail of the data for high values of ω , the 2p2h coefficients now being adjustable parameters to describe the tail of the scaling function.

To obtain the scaled data, we divide the cross section by the averaged single nucleon response. By doing so, we can assume that the 2p2h component of the scaling function arises from the 2p2h emission induced by the one-body current. This assumption is based on the observation that the 2p2h-like contribution captures the high-energy tail of the data. By parametrizing the scaling function in this way, we are able to disentangle the 2p2h contribution from the 1p1h one and extract information about the underlying dynamics of the reaction. This allows us to investigate the role of 2p2h processes induced by the one-body current and their impact on the scaling behavior observed in the experimental data.

In the SuSAM* approach the superscaling analysis of electron scattering data is used to predict QE neutrino-nucleus cross sections [42]. The neutrino (antineutrino) cross section was extended to the 2p2h sector with a relativistic MEC operator in the RMF model of nuclear matter [23], where the semiempirical formula for two-nucleon emission responses was fitted to the exact results for momenta in the range $q = 200$ and 2000 MeV/c. The semiempirical formula allows to compute accurately the

2p2h MEC responses using an analytical formula, thus reducing the calculation time. Similarly, in this work, we extend the new parametrization of the scaling function to the case of neutrino scattering. We use the same 2p2h parameters obtained from electron scattering, but multiply them by the weak responses of a nucleon instead of the electromagnetic responses. By applying this approach to neutrino scattering, we aim to investigate the role of 2p2h processes induced by the weak one-body current and their contribution to the charged-current (CC) neutrino cross section. By utilizing the same 2p2h parameters, we can effectively compare the 2p2h contributions in electron and neutrino scattering and assess the universality of the scaling behavior across different interaction channels.

The scheme of the paper is as follows. In Sect. II we present the superscaling formalism. In sect. III we study the particular case of the correlation current in the independent pair approximation. In sect. IV we introduce the semiempirical formula for the 2p2h response function induced by the OB current. In sect. V we presents the results. Finally, in Sect. VI we draw our conclusions.

II. FORMALISM

We follow the formalism of Ref. [2]. We start with the inclusive electron scattering cross section in plane-wave Born approximation with one photon-exchange

$$\frac{d\sigma}{d\Omega d\epsilon'} = \sigma_{\text{Mott}}(v_L R_L(q, \omega) + v_T R_T(q, \omega)), \quad (1)$$

where the incident electron has energy ϵ , the scattering angle is θ , the final energy is energy ϵ' , and Ω is the solid angle for the electron detection. The energy transfer is $\omega = \epsilon - \epsilon'$, the momentum transfer is \mathbf{q} . In Eq. (1) σ_{Mott} is the Mott cross section, v_L and v_T are kinematic factors coming from the leptonic tensor

$$v_L = \frac{Q^4}{q^4}, \quad v_T = \tan^2 \frac{\theta}{2} - \frac{Q^2}{2q^2}. \quad (2)$$

Finally, the longitudinal and transverse response functions, only depend on (q, ω) and are the following components of the hadronic tensor

$$R_L(q, \omega) = W^{00}, \quad R_T(q, \omega) = W^{11} + W^{22}, \quad (3)$$

where $W^{\mu\nu}$ is the nuclear hadronic tensor, see Ref. [2] for details.

In refs. [22, 23] we developed a model of the reaction where the responses are the sum of QE plus 2p2h MEC contribution

$$R_K(q, \omega) = R_K^{QE}(q, \omega) + R_K^{MEC}(q, \omega) + \dots, \quad (4)$$

for $K = L, T$, where contributions of pion emission, and beyond are not included in our model. The MEC responses were studied in detail in [23], where a semiempirical formula was derived from a microscopical relativistic

current in the RMF model of nuclear matter. We focus in this work on the QE responses that we describe using the SuSAM* approach [22, 41]. This model is an extension of the RMF model of nuclear matter [8], where the initial and final nucleons are interacting with the nuclear mean field and acquire an effective mass m_N^* . The 1p1h response functions are

$$R_K^{QE}(q, \omega) = \frac{V}{(2\pi)^3} \int d^3h \frac{(m_N^*)^2}{EE'} \delta(E' - E - \omega) \times \theta(p' - k_F) \theta(k_F - h) 2U_K. \quad (5)$$

The initial nucleon has momentum \mathbf{h} below the Fermi momentum, $h < k_F$, and on-shell energy $E = \sqrt{\mathbf{h}^2 + m_N^{*2}}$. The final nucleon has momentum $\mathbf{p}' = \mathbf{h} + \mathbf{q}$, and the final on-shell energy is $E' = \sqrt{\mathbf{p}'^2 + m_N^{*2}}$. Pauli blocking implies $p' > k_F$. The U_K are the single-nucleon responses for the 1p1h excitation

$$U_L = w^{00}, \quad U_T = w^{11} + w^{22}, \quad (6)$$

corresponding to the single-nucleon hadronic tensor

$$w^{\mu\nu} = \frac{1}{2} \sum_{ss'} j_{OB}^\mu(\mathbf{p}', \mathbf{h})_{s's}^* j_{OB}^\nu(\mathbf{p}', \mathbf{h})_{s's} \quad (7)$$

and j_{OB}^μ is the electromagnetic current matrix element

$$j_{OB}^\mu(\mathbf{p}', \mathbf{h})_{s's} = \bar{u}(\mathbf{p}')_{s'} \left[F_1 \gamma^\mu + i \frac{F_2}{2m_N} \sigma^{\mu\nu} Q_\nu \right] u(\mathbf{h})_s, \quad (8)$$

where F_1 and F_2 , are the Dirac and Pauli form factors. To compute the integral of Eq. (5), the usual procedure is to change from variable θ_h to E' . The integral over E' is made using the Dirac delta, this fixes the value of the angle between \mathbf{h} and \mathbf{q} , $\cos\theta_h = (2E\omega + Q^2)/(2hq)$, and the integration over the azimuthal angle ϕ gives 2π by symmetry of the responses when \mathbf{q} is on the z -axis [2]. We are left with an integral over the initial nucleon energy

$$R_K^{QE}(q, \omega) = \frac{V}{(2\pi)^3} \frac{2\pi m_N^{*3}}{q} \int_{\epsilon_0}^{\infty} d\epsilon n(\epsilon) 2U_K(\epsilon, q, \omega), \quad (9)$$

where $\epsilon = E/m_N^*$ is the initial nucleon energy in units of m_N^* , and $\epsilon_F = E_F/m_N^*$ is the (relativistic) Fermi energy in the same units. Moreover we have introduced the energy distribution of the Fermi gas $n(\epsilon) = \theta(\epsilon_F - \epsilon)$. The lower limit, ϵ_0 of the integral in Eq. (9) corresponds to the minimum energy for a initial nucleon that absorbs energy ω and momentum q . It can be written as (see Appendix C of ref. [2])

$$\epsilon_0 = \text{Max} \left\{ \kappa \sqrt{1 + \frac{1}{\tau}} - \lambda, \epsilon_F - 2\lambda \right\}, \quad (10)$$

where we have introduced the dimensionless variables

$$\lambda = \omega/2m_N^*, \quad \kappa = q/2m_N^*, \quad \tau = \kappa^2 - \lambda^2. \quad (11)$$

Now we define a mean value of the single-nucleon responses [43] by averaging with the energy distribution $n(\epsilon)$

$$\bar{U}_K(q, \omega) = \frac{\int_{\epsilon_0}^{\infty} d\epsilon n(\epsilon) U_K(\epsilon, q, \omega)}{\int_{\epsilon_0}^{\infty} d\epsilon n(\epsilon)}. \quad (12)$$

Using these averaged single-nucleon responses we can rewrite Eq. (9) in the form

$$R_K^{QE}(q, \omega) = \frac{V}{(2\pi)^3} \frac{2\pi m_N^{*3}}{q} 2\bar{U}_K \int_{\epsilon_0}^{\infty} d\epsilon n(\epsilon). \quad (13)$$

The superscaling function is defined as

$$\frac{4}{3} \xi_F f^*(\psi^*) = \int_{\epsilon_0}^{\infty} n(\epsilon) d\epsilon, \quad (14)$$

where $\xi_F = \epsilon_F - 1 \ll 1$ is the kinetic Fermi energy in units of m_N^* . Note that this integral only depends on the variable ϵ_0 , which in turn depends on (q, ω) . The definition (14) is, except for a factor, similar to that of the y -scaling function $f(y)$ [44, 45], where the scaling variable y was the minimum momentum of the initial nucleon. In this paper we use the ψ^* -scaling variable. The minimum energy of the nucleon, ϵ_0 , is transformed by a change of variable into the scaling variable, ψ^* , defined as

$$\psi^* = \sqrt{\frac{\epsilon_0 - 1}{\epsilon_F - 1}} \text{sgn}(\lambda - \tau). \quad (15)$$

In relativistic Fermi gas (RFG) and in nuclear matter with RMF $1 \leq \epsilon_0 \leq \epsilon_F$ and consequently the RFG superscaling function is zero outside this interval, that corresponds to $1 < |\psi^*|$ for all nuclei. However, in a real nucleus the momentum is not limited by k_F , since nucleons can have higher momentum, especially correlated nucleons can greatly exceed the Fermi momentum. This has the effect that the phenomenological superscaling function is not zero for $|\psi^*| > 1$. Equivalently, the high-energy tail of the phenomenological scaling function, for $\psi > 1$, can be described as a consequence of two-particle emission induced by the one-body current. This means that the observed asymmetry in the scaling function can be attributed to the contribution of two-particle emission processes.

Using $V/(2\pi)^3 = N/(\frac{8}{3}\pi k_F^3)$ we can write

$$R_K^{QE} = \frac{\xi_F}{m_N^* \eta_F^3 \kappa} (Z \bar{U}_K^p + N \bar{U}_K^n) f^*(\psi^*), \quad (16)$$

where we have added the contribution of Z protons and N neutrons to the response functions, and $\eta_F = k_F/m_N^*$. The SuSAM* approach, extends the formula (16) using a phenomenological scaling function, obtained from experimental data of (e, e') . In the SuSAM* of ref. [22] the 2p2h contribution of MEC was first subtracted from the inclusive cross section and then divided by the contribution of the single nucleon.

$$f_{QE}^* = \frac{(\frac{d\sigma}{d\Omega d\omega})_{exp} - (\frac{d\sigma}{d\Omega d\omega})_{MEC}}{\sigma_M(v_L r_L + v_T r_T)}, \quad (17)$$

where

$$r_K = \frac{\xi_F}{m_N^* \eta_F^3 \kappa} (Z \bar{U}_K^p + N \bar{U}_K^n). \quad (18)$$

Second a selection of the QE data points was done by noting that approximately half of the data collapse into a point cloud around the RFG scaling function. This point cloud constitutes the data that can be considered approximately QE and we reject the rest, which contribute to inelastic processes. Examples of the selected QE data are shown in Figs. 1 and 2. In these figures, it is evident that the scaled quasielastic data cluster together, forming an asymmetric thick band that exhibits a tail for high energies. In the results section, we will show that this tail can be parametrized with a function that is proportional to the 2p2h phase space.

III. 2P2H RESPONSE FUNCTIONS WITH CORRELATED PAIRS

Before introducing our parameterization of the 2p2h response due to the OB current, we first investigate the expected structure of the 2p-2h response functions in a simple model. In this model, the OB current induces two-particle emission when acting on the wave function of a correlated pair of nucleons. This is expected to be one of the contributions to the 2p2h response, although not the only one. In this section, other effects, such as interference with the two-body current, are not considered.

Our theoretical motivation is based on the RFG and the independent pair approximation or Bethe-Goldstone equation for the wave function of a pair of correlated nucleons in presence of the nuclear medium. Our aim is not to develop a detailed and exhaustive microscopic model, but rather to provide some basic outlines in a schematic model, as a starting point for proposing a formula that accounts for the fundamental ingredients that determine the 2p2h response.

For convenience we use here square brackets in the notation of normalized states within the volume box V , indicating that the states are normalized to unity within the box

$$|[\mathbf{p}]\rangle \equiv \frac{e^{i\mathbf{p}\cdot\mathbf{r}}}{\sqrt{V}} |\frac{1}{2}s\rangle \otimes |\frac{1}{2}t\rangle, \quad (19)$$

while the absence of brackets indicates that the states are normalized over the entire space to a Dirac's delta of momentum, i.e.

$$|\mathbf{p}\rangle \equiv \frac{e^{i\mathbf{p}\cdot\mathbf{r}}}{(2\pi)^{3/2}} |\frac{1}{2}s\rangle \otimes |\frac{1}{2}t\rangle \quad (20)$$

The previous states carry implicit spin and isospin indices, which we do not write for convenience and to keep the equations short in order to enhance clarity.

In the absence of correlations, the only mechanism of interaction that can excite a 2p2h state is a two-body current, particularly meson exchange currents, whose matrix elements in the RFG can be written as:

$$\langle [\mathbf{p}'_1 \mathbf{p}'_2] | J^\mu(\mathbf{q}, \omega) | [\mathbf{h}_1 \mathbf{h}_2] \rangle = \frac{(2\pi)^3}{V^2} \delta(\mathbf{p}'_1 + \mathbf{p}'_2 - \mathbf{q} - \mathbf{h}_1 - \mathbf{h}_2) j^\mu(\mathbf{p}'_1, \mathbf{p}'_2, \mathbf{h}_1, \mathbf{h}_2). \quad (21)$$

where $p'_i > k_F$ and $h_i < k_F$. The two-body current functions $j^\mu(\mathbf{p}'_1, \mathbf{p}'_2, \mathbf{h}_1, \mathbf{h}_2)$ also depends implicitly on spin-isospin indices.

The corresponding inclusive hadronic tensor in the 2p2h channel can be written as

$$\begin{aligned} W_{2p2h}^{\mu\nu}(q, \omega) &= \frac{V}{(2\pi)^9} \int d^3p'_1 d^3p'_2 d^3h_1 d^3h_2 \frac{(m_N^*)^4}{E_1 E_2 E'_1 E'_2} \\ &\times w^{\mu\nu}(\mathbf{p}'_1, \mathbf{p}'_2, \mathbf{h}_1, \mathbf{h}_2) \\ &\times \theta(p'_1 - k_F^N) \theta(k_F^N - h_1) \theta(p'_2 - k_F^N) \theta(k_F^N - h_2) \\ &\times \delta(E'_1 + E'_2 - E_1 - E_2 - \omega) \\ &\times \delta(\mathbf{p}'_1 + \mathbf{p}'_2 - \mathbf{q} - \mathbf{h}_1 - \mathbf{h}_2), \end{aligned} \quad (22)$$

where E_i, E'_i are the on-shell energies of nucleons with momenta $\mathbf{h}_i, \mathbf{p}'_i$, and with relativistic effective mass m_N^* . The function $w^{\mu\nu}(\mathbf{p}'_1, \mathbf{p}'_2, \mathbf{h}_1, \mathbf{h}_2)$ represents the hadron tensor for a single 2p2h transition, summed up over spin and isospin,

$$\begin{aligned} w^{\mu\nu}(\mathbf{p}'_1, \mathbf{p}'_2, \mathbf{h}_1, \mathbf{h}_2) &= \\ &= \frac{1}{4} \sum_{s_1 s_2 s'_1 s'_2} \sum_{t_1 t_2 t'_1 t'_2} j^\mu(1', 2', 1, 2)_A^* j^\nu(1', 2', 1, 2)_A. \end{aligned} \quad (23)$$

where the two-body current function is antisymmetrized

$$j^\mu(1', 2', 1, 2)_A \equiv j^\mu(1', 2', 1, 2) - j^\mu(1', 2', 2, 1). \quad (24)$$

The factor 1/4 in Eq. (23) accounts for the anti-symmetry of the two-body wave function with respect to exchange of momenta, spin and isospin quantum numbers, to avoid double counting of the final 2p2h states.

Let's now consider the matrix element of the one-body current $J^\mu(\mathbf{q}, \omega) = J_{OB}^\mu = \sum_i J_i^\mu$, where the J_i^μ acts on the i -th particle. We have

$$\langle \mathbf{p}'_1 \mathbf{p}'_2 | J_{OB}^\mu | \mathbf{h}_1 \mathbf{h}_2 \rangle = \langle \mathbf{p}'_1 \mathbf{p}'_2 | J_1^\mu + J_2^\mu | \mathbf{h}_1 \mathbf{h}_2 \rangle = 0 \quad (25)$$

Indeed, a one-body current cannot produce 2p2h excitations due to the orthogonality of plane waves $\langle \mathbf{p}'_i | \mathbf{h}_j \rangle = 0$.

The situation changes when we consider that the two states $|\mathbf{h}_i\rangle$ are interacting in the medium, with a short-range NN potential V_{NN} that produces scattering to unoccupied states. If we turn-on the NN interaction the wave function $|\mathbf{h}_1 \mathbf{h}_2\rangle$ of the pair is modified, but due to Pauli blocking it can only acquire momentum components above the Fermi momentum. In the independent pair approximation the wave function $|\mathbf{h}_1 \mathbf{h}_2\rangle$ is replaced by the correlated wave function $|\Phi_{\mathbf{h}_1 \mathbf{h}_2}\rangle$

$$|\mathbf{h}_1, \mathbf{h}_2\rangle \rightarrow |\Phi_{\mathbf{h}_1 \mathbf{h}_2}\rangle = |\mathbf{h}_1, \mathbf{h}_2\rangle + |\Delta\Phi_{\mathbf{h}_1 \mathbf{h}_2}\rangle \quad (26)$$

where $|\Delta\Phi_{\mathbf{h}_1\mathbf{h}_2}\rangle$ only has high momentum components. In the independent pair approximation the wave function is obtained from the solution of the BG equation for the correlated wave function [46]. Since the NN interaction conserves the total momentum, the correlated part of the wave function in momentum space verifies

$$\langle \mathbf{p}_1\mathbf{p}_2 | \Delta\Phi_{\mathbf{h}_1\mathbf{h}_2} \rangle = \delta(\mathbf{p}_1 + \mathbf{p}_2 - \mathbf{h}_1 - \mathbf{h}_2) \Delta\varphi_{\mathbf{h}_1\mathbf{h}_2}(\mathbf{p}) \quad (27)$$

where $\mathbf{p} = \frac{1}{2}(\mathbf{p}_1 - \mathbf{p}_2)$ is the relative momentum of the nucleon pair, and $\Delta\varphi_{\mathbf{h}_1\mathbf{h}_2}(\mathbf{p})$ is the relative wave function of $\Delta\Phi_{\mathbf{h}_1\mathbf{h}_2}$. From the BG equation, it is given by [47]

$$\Delta\varphi_{\mathbf{h}_1\mathbf{h}_2}(\mathbf{p}) = \frac{\theta(p_1 - k_F)\theta(p_2 - k_F)}{h^2 - p^2} \langle \mathbf{p} | 2\mu V_{NN} | \varphi_{\mathbf{h}_1\mathbf{h}_2} \rangle \quad (28)$$

where $\varphi_{\mathbf{h}_1\mathbf{h}_2}(\mathbf{p})$ is the relative wave function of $\Phi_{\mathbf{h}_1\mathbf{h}_2}$, $\mu = \frac{m_N}{2}$ is the reduced mass of the two-nucleon system and $\mathbf{h} = (\mathbf{h}_1 - \mathbf{h}_2)/2$ the initial relative momentum, while $\mathbf{p}_1 = (\mathbf{h}_1 + \mathbf{h}_2)/2 + \mathbf{p}$ and $\mathbf{p}_2 = (\mathbf{h}_1 + \mathbf{h}_2)/2 - \mathbf{p}$. The Pauli blocking functions in Eq. (28) ensure that the wave function has high-momentum components. As we can see, it is not possible to remove the dependence on the total momentum $\mathbf{h}_1 + \mathbf{h}_2$ appearing in the Pauli-blocking step functions. Therefore a dependence of short-range correlations on the CM momentum of the pair appears.

Now, by applying a one-body current to a system of two correlated nucleons, it is possible to generate a two-particle state that exists above the Fermi level. The 2p-2h matrix element of the one-body current is computed in Appendix A. It can be written similarly to Eq. (21)

$$\langle [\mathbf{p}'_1\mathbf{p}'_2] | J_{OB}^\mu(\mathbf{q}) | [\Phi_{\mathbf{h}_1\mathbf{h}_2}] \rangle = \frac{(2\pi)^3}{V^2} \delta(\mathbf{p}'_1 + \mathbf{p}'_2 - \mathbf{q} - \mathbf{h}_1 - \mathbf{h}_2) j_{cor}^\mu(\mathbf{p}'_1, \mathbf{p}'_2, \mathbf{h}_1, \mathbf{h}_2). \quad (29)$$

It is noteworthy that the matrix element describing the effect of the one-body current on the wave function of two correlated nucleons is formally similar to the matrix element of a two-body correlation current, which is represented by the function j_{cor}^μ

$$j_{cor}^\mu(\mathbf{p}'_1, \mathbf{p}'_2, \mathbf{h}_1, \mathbf{h}_2) = (2\pi)^3 j_{OB}^\mu(\mathbf{p}'_1, \mathbf{p}'_1 - \mathbf{q}) \Delta\varphi_{\mathbf{h}_1\mathbf{h}_2}(\mathbf{p}' - \frac{\mathbf{q}}{2}) + (2\pi)^3 j_{OB}^\mu(\mathbf{p}'_2, \mathbf{p}'_2 - \mathbf{q}) \Delta\varphi_{\mathbf{h}_1\mathbf{h}_2}(\mathbf{p}' + \frac{\mathbf{q}}{2}) \quad (30)$$

where $\mathbf{p}' = (\mathbf{p}'_1 - \mathbf{p}'_2)/2$ is the relative momentum of the final particles.

The correlation current is the sum of the products of the OB current multiplied by the high-momentum wave function of the initial correlated pair. This is illustrated in the diagrams of Fig. 1. The shaded rectangle represents the correlations resulting in the production of high-momentum components of the correlated pair $(\mathbf{h}_1, \mathbf{h}_2)$. One of the high-momentum nucleons absorbs a photon with momentum q , while the other nucleon is emitted through its interaction with the first nucleon. In Eq. (30) the products are, in fact, a multiplication of spin

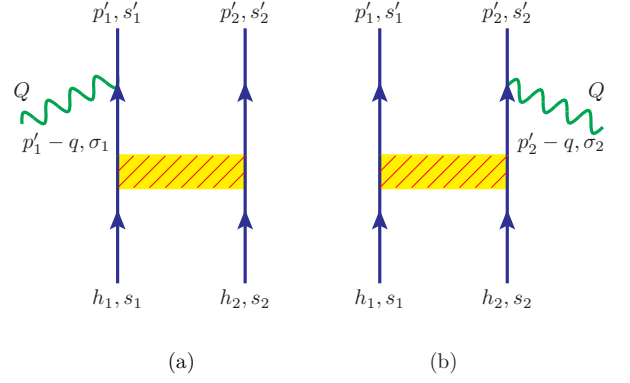


FIG. 1: Diagram illustrating the correlation current, Eq (30). The spins of the final particles are s'_1 and s'_2 , whereas σ_1, σ_2 denotes one of the spin components of the relative wave function of high momentum, represented by the shaded rectangle.

matrices, although we have left this out of equation (30) for clarity. The complete formula dependent on spin is provided in the appendix A, Eq. (A8). Note also that the current depends on isospin. Hence, when the initial state consists of a proton-neutron pair, the current acting on the first particle must correspond to the proton current, while the current acting on the second particle should correspond to the neutron current.

By inserting the correlation current (30) in Eq. (23) the hadronic tensor for a 2p2h transition is obtained. The isospin sums in Eq. (23) can be written as sums over pp, pn, and nn correlated pairs. Therefore

$$w^{\mu\nu}(\mathbf{p}'_1, \mathbf{p}'_2, \mathbf{h}_2, \mathbf{h}_2) = w_{pp}^{\mu\nu} + w_{np}^{\mu\nu} + w_{nn}^{\mu\nu}. \quad (31)$$

Writing explicitly the isospin indices, $N, N' = p, n$, the diagonal components of the hadronic tensor $w_{NN'}^{\mu\nu}$ are the following

$$w_{NN'}^{\mu\nu}(\mathbf{p}'_1, \mathbf{p}'_2, \mathbf{h}_1, \mathbf{h}_2) = (2\pi)^6 \left| j_N^\mu(\mathbf{p}'_1, \mathbf{p}'_1 - \mathbf{q}) \Delta\varphi_{\mathbf{h}_1\mathbf{h}_2}^{NN'}(\mathbf{p}' - \frac{\mathbf{q}}{2}) \right|^2 + (2\pi)^6 \left| j_{N'}^\mu(\mathbf{p}'_2, \mathbf{p}'_2 - \mathbf{q}) \Delta\varphi_{\mathbf{h}_1\mathbf{h}_2}^{NN'}(\mathbf{p}' + \frac{\mathbf{q}}{2}) \right|^2 + 2(2\pi)^6 \text{Re} \left\{ j_N^{\mu*}(\mathbf{p}'_1, \mathbf{p}'_1 - \mathbf{q}) \Delta\varphi_{\mathbf{h}_1\mathbf{h}_2}^{NN'*}(\mathbf{p}' - \frac{\mathbf{q}}{2}) \times j_{N'}^\mu(\mathbf{p}'_2, \mathbf{p}'_2 - \mathbf{q}) \Delta\varphi_{\mathbf{h}_1\mathbf{h}_2}^{NN'}(\mathbf{p}' + \frac{\mathbf{q}}{2}) \right\} \quad (32)$$

In the independent pair approximation the 2p2h hadronic tensor $W_{NN'}^{\mu\nu}(q, \omega)$ due to SRC, is defined as the integral of the correlated-pair tensor $w_{NN'}^{\mu\nu}(\mathbf{p}'_1, \mathbf{p}'_2, \mathbf{h}_2, \mathbf{h}_2)$ over the momentum space of 2p2h excitations, using Eq. (22). The computation of this tensor falls outside the scope of the present work. The proposed approach for such a calculation would require solving the Bethe-Goldstone equation for every nucleon pair $\mathbf{h}_1, \mathbf{h}_2$ while considering the center of mass of the two particles $\mathbf{h}_1 + \mathbf{h}_2 \neq 0$, and performing a seven-dimensional integration. In reference [47], the BG equation was solved for the particular case of back-to-back

nucleons, $\mathbf{h}_1 + \mathbf{h}_2 = 0$, moving along the z -axis in a multipole expansion with a potential V_{NN} fitted to NN scattering data [48]. Although the computation seems feasible, incorporating the center of mass for particles moving in any direction requires careful consideration of various technical details.

The phenomenological approach of scaling analysis relies on the factorization approximation of the single-nucleon response. In the subsequent section, we will explore the consequences of adopting this approximation in the model introduced in the current section. We will further generalize it to derive an empirical factorized formula that can be applied within the scaling approach. However, it is important to note that the factorization approximation is a simplification and may overlook certain many-body effects that can play a role in the response. Therefore, the empirical factorized formula should be seen as an approximation that captures the main trends observed in the scaling behavior rather than a complete microscopic description.

IV. SEMIEMPIRICAL 2P2H RESPONSE FUNCTIONS

The 2p2h response functions for two-body operators (MEC) was explored in Ref. [23]. Our analysis revealed that the responses of a pair can be factorized out of the integral (22) with reasonable approximation. By doing so, we derived a semi-empirical expression for the MEC responses, with the coefficients to be determined by later fitting. In this work, we make the assumption that a similar factorization occurs for the 2p2h response induced by the one-body (OB) current. This implies that the 2p2h response can be proportional to the phase-space integral of two nucleons. In the framework of the RMF of nuclear matter the 2p2h phase-space function is given by the integral

$$\begin{aligned}
 F_{NN'}(q, \omega) = & \int d^3p'_1 d^3p'_2 d^3h_1 d^3h_2 \frac{(m_N^*)^4}{E_1 E_2 E'_1 E'_2} \\
 & \times \theta(p'_1 - k_F^N) \theta(k_F^N - h_1) \theta(p'_2 - k_F^{N'}) \theta(k_F^{N'} - h_2) \\
 & \times \delta(E'_1 + E'_2 - E_1 - E_2 - \omega) \\
 & \times \delta(\mathbf{p}'_1 + \mathbf{p}'_2 - \mathbf{q} - \mathbf{h}_1 - \mathbf{h}_2), \quad (33)
 \end{aligned}$$

where N , N' can be proton or neutron, depending on the initial correlated state pp, pn or nn and k_F^N is the Fermi momentum of the nucleon of N kind. The phase space function is roughly proportional to the number of 2p2h excitations allowed by the kinematic for momentum and energy transfer (q, ω) .

The concept of factorization in the 2p2h channel bears some resemblance to that employed in the 1p1h channel, where the response was written as a single-nucleon averaged response multiplied by the superscaling function. In the 2p2h case, we will also define the two-nucleon tensor averaged over the momentum space of 2p2h excitations, by dividing the hadronic tensor over the phase

space function as follows

$$\overline{w}_{NN'}^{\mu\nu}(q, \omega) \equiv \frac{W_{NN'}^{\mu\nu}(q, \omega)}{\frac{V}{(2\pi)^9} F_{NN'}(q, \omega)} \quad (34)$$

In the definition given in Eq. (34) $W_{NN'}^{\mu\nu}(q, \omega)$ can be in general the exact hadronic tensor for 2p2h emission including the one-body current and possibly other interference contributions, not only the correlations. This leads to an exact factorization of the 2p2h hadronic tensor as the averaged two-nucleon tensor multiplied by the phase space.

$$W_{NN'}^{\mu\nu}(q, \omega) = \frac{V}{(2\pi)^9} F_{NN'}(q, \omega) \overline{w}_{NN'}^{\mu\nu}(q, \omega) \quad (35)$$

In this formula the averaged two-nucleon tensor accounts for the correlations and other interaction contributions such as interferences with the two-body current, while the phase space does not contain any information about them. The phase space is exclusively related to the kinematics of independent particles without interactions in the Fermi gas.

To proceed further, we analyze the specific case of the hadronic tensor in the model of independent pairs that was introduced in the previous section. The average of the tensor $w_{NN'}^{\mu\nu}$ in equation (32) is typically complicated. Two approximations lead to the simplification of this term. We will make the assumption that the average of the product can be written as the product of averages, and neglect on the average the interference term between the two particles, given by the last term in Eq. (32). In this way we obtain for the diagonal components

$$\overline{w}_{NN'}^{\mu\mu}(q, \omega) \simeq (2\pi)^6 \left(\overline{|j_N^\mu|^2} + \overline{|j_{N'}^\mu|^2} \right) \times \overline{|\Delta\varphi_{\mathbf{h}_1\mathbf{h}_2}^{NN'}|^2}, \quad (36)$$

where we use the notation

$$\overline{|j_N^\mu|^2} \equiv \overline{|j_N^\mu(\mathbf{p}'_1, \mathbf{p}'_1 - \mathbf{q})|^2} = \overline{|j_N^\mu(\mathbf{p}'_2, \mathbf{p}'_2 - \mathbf{q})|^2} \quad (37)$$

$$\begin{aligned}
 \overline{|\Delta\varphi_{\mathbf{h}_1\mathbf{h}_2}^{NN'}|^2} & \equiv \overline{\left| \Delta\varphi_{\mathbf{h}_1\mathbf{h}_2}^{NN'} \left(\mathbf{p}' + \frac{\mathbf{q}}{2} \right) \right|^2} \\
 & = \overline{\left| \Delta\varphi_{\mathbf{h}_1\mathbf{h}_2}^{NN'} \left(\mathbf{p}' - \frac{\mathbf{q}}{2} \right) \right|^2}. \quad (38)
 \end{aligned}$$

Therefore, by performing the factorization approximation of the OB current in the independent-pair model and neglecting the interferences, we find that the corresponding hadronic tensor, based on Eqs (35,36), includes the product of three factors: the 2p2h phase-space integral, the averaged response of a single nucleon (coming from the one-body current), and a factor related to the averaged high-momentum distribution of a pair. In the semiempirical formula for the 2p2h response we assume the same factorization, we will replace this factor with an adjustable parameter that is not necessarily associated solely with correlations, as it will include contributions and interferences with other processes, particularly

MEC. Hence, we propose the following semi-empirical formula for the 2p2h responses induced by the OB current in electron scattering.

$$R_{2p2h}^K = \frac{V}{(2\pi)^9} \frac{1}{m_N^2 m_\pi^4} \frac{2}{A(A-1)} \times \left[\frac{Z(Z-1)}{2} F_{pp}(q, \omega) c_K^{pp}(q) (2\bar{U}_K^p) + NZ F_{pn}(q, \omega) c_K^{pn}(q) (\bar{U}_K^p + \bar{U}_K^n) + \frac{N(N-1)}{2} F_{nn}(q, \omega) c_K^{nn}(q) (2\bar{U}_K^n) \right]. \quad (39)$$

The mass of the pion (m_π)⁴ in the denominator has been introduced for convenience by analogy to MEC responses [23] and the mass of the nucleon m_N^2 in the denominator is set so that the 2p2h parameters $c_K^{NN'}(q)$ are dimensionless.

In Eq. (39), we have separated the contributions of the pairs, pp, pn and nn. Each of them is proportional to the sum of the corresponding single-nucleon responses, \bar{U}_K^p and/or \bar{U}_K^n . This is because the photon can be absorbed by both nucleons of the pair. Also, each contribution has been multiplied by the number of pairs pp, pn or nn and divided by the total number of pairs, $A(A-1)/2$, to take into account asymmetric matter $Z \neq N$. This approach follows the lines of the model of ref. [38].

Since we expect that the 2p2h parameters $c_K(q)$ are related, at least partially, to the high momentum components of a nucleon pair, they should strongly depend on isospin, given that the high momentum components of proton-neutron dominate over proton-proton and neutron-neutron. Here we will assume that they are proportional $c_K^{pp}(q) = c_K^{nn}(q) = \alpha c_K^{pn}(q)$, where α is a small constant. Experiments on ¹²C have reported a number of np pairs 18 times larger than their pp counterparts [49, 50]. Then a reasonable value is $\alpha = 1/18$.

It is also reasonable to assume that the $c_K^{NN'}$ coefficients are the same for both the longitudinal and transverse response, $c_L^{NN'} = c_T^{NN'} = c^{NN'}$. This assumption greatly simplifies the semiempirical formula because it only depends on two parameters c^{pn} and α . It is important to note that this assumption may not hold true in all cases, and care should be taken when interpreting results obtained using this simplification.

In the particular case of the factorized independent-pair model neglecting the interferences, based on the equation (36), the 2p2h parameter $c^{pn}(q)$ is related to the average momentum distribution of a proton-neutron pair in the 2p2h excitation

$$\frac{c^{pn}(q)}{m_N^2 m_\pi^4} \simeq (2\pi)^6 \left(\sum_{s_1 s_2 s'_1 s'_2} |\Delta \varphi_{\mathbf{h}_1 \mathbf{h}_2}^{pn}(\mathbf{p}' + \mathbf{q}/2)|^2 \right). \quad (40)$$

However, in the real case, this may not necessarily hold true because there are other mechanisms to consider, such as interference with two-body currents, FSI, etc.

Therefore, in the present phenomenological approach, the 2p2h parameters are considered as adjustable quantities to reproduce the tail of the scaling function. In other words, they quantify to some extent the asymmetry of the phenomenological scaling function (see next section).

In the case of symmetric nuclei, $N = Z$, Eq. (39) reduces to

$$R_{2p2h}^K = \frac{V}{(2\pi)^9} F(q, \omega) \frac{Z + \alpha(Z-1)}{2Z-1} \frac{c^{pn}(q)}{m_N^2 m_\pi^4} (\bar{U}_K^p + \bar{U}_K^n). \quad (41)$$

From the response functions we can write the semiempirical formula for the inclusive cross section in the 2p2h channel induced by the one-body current

$$\left(\frac{d\sigma}{d\Omega' d\epsilon'} \right)_{2p2h}^{em} = \frac{\sigma_{\text{Mott}} V}{(2\pi)^9} \frac{F(q, \omega) c^{pn}(q)}{m_N^2 m_\pi^4} \frac{Z + \alpha(Z-1)}{2Z-1} \left[v_L (\bar{U}_L^p + \bar{U}_L^n) + v_T (\bar{U}_T^p + \bar{U}_T^n) \right]. \quad (42)$$

In the next section we use the ¹²C(e, e') cross section data to fit the 2p2h parameter $c^{pn}(q)$ for each q .

In the case of CC neutrino scattering the semiempirical formula extends naturally by replacing the electromagnetic single nucleon responses with the corresponding to the $n(\nu_\mu, \mu)p$ or $p(\bar{\nu}_\mu, \mu^+)n$, assuming the same relation between the 2p2h parameters of the nn and pp in the case of anti-neutrino pairs to the np pairs in the initial state $c^{nn} = c^{pp} = \alpha c^{pn}$

$$\left(\frac{d\sigma}{d\Omega' d\epsilon'} \right)_{2p2h}^\nu = \frac{\sigma_0 V}{(2\pi)^9} \frac{F(q, \omega) c^{pn}(q)}{m_N^2 m_\pi^4} \frac{Z + \alpha(Z-1)}{2Z-1} \left[V_{CC} \bar{U}_{CC} + 2V_{CL} \bar{U}_{CL} + V_{LL} \bar{U}_{LL} + V_T \bar{U}_T \pm 2V_{T'} \bar{U}_{T'} \right], \quad (43)$$

where σ_0 is

$$\sigma_0 = \frac{G^2 \cos^2 \theta_c}{4\pi^2} \frac{k'}{\epsilon} [(\epsilon + \epsilon')^2 - q^2], \quad (44)$$

with G the Fermi constant and θ_c the Cabibbo angle. The lepton coefficients for neutrino scattering V_K are given in Ref. [2]. The average single nucleon responses \bar{U}_K are given in Appendix B. Here we use a new version of these responses using the definition (12) with the distribution $n(\epsilon)$ obtained from the phenomenological scaling function. This differs from the traditional definition [42] only for $\psi > 1$, where the contribution of the nucleons with momentum greater than k_F is correctly taken into account, while the traditional definition is an extrapolation of the RFG where the nucleons are limited by k_F [43].

Finally, in the semi-empirical formula will make use of the following approximation for the phase-space function [53]:

$$F_{NN'}(q, \omega) = \left(4\pi k_F^N k_F^{N'} \right)^3 \frac{m_N^{*2}}{18} \sqrt{1 - \frac{4m_N^{*2}}{(2m_N^* + \omega)^2 - q^2}}. \quad (45)$$

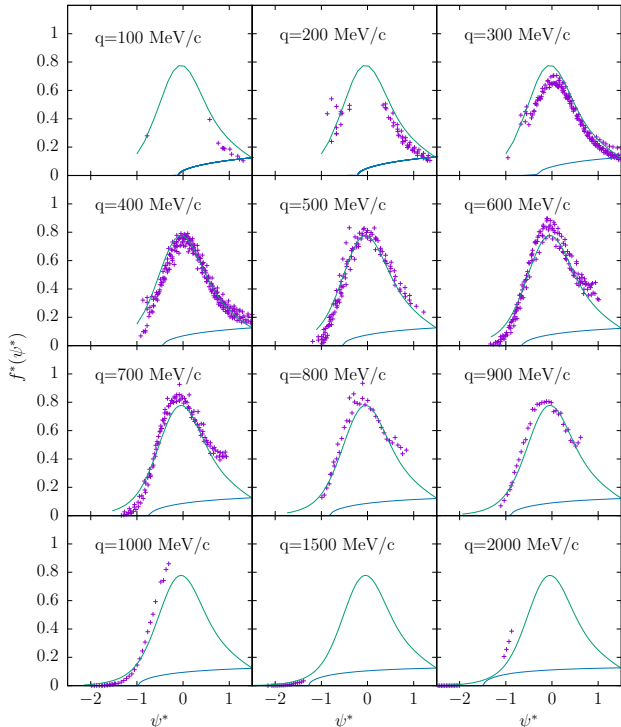


FIG. 2: Scaling function of the SuSAM* model (green) compared to the contribution f_{2p2h}^* in the 2p2h channel (blue) for several values of q , as a function of the scaling variable ψ^* . For each q we show only the scaled ^{12}C data for $q \pm 50$ MeV/c. The original data are taken from [51, 52]

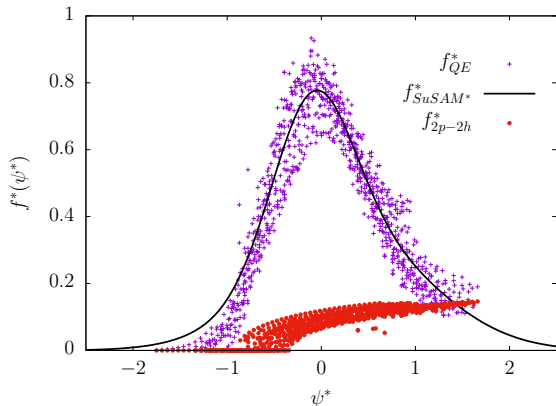


FIG. 3: Experimental data of the scaling function f_{QE}^* compared to the 2p2h contribution. Only data with $q \leq 1000$ MeV/c are shown. The solid line is the SuSAM* fit.

Eq. (45) makes use of the frozen nucleon approximation to compute the integral (33). The exact phase space was studied in depth in ref [54] as a function of (q, ω) for the kinematics of interest for neutrino experiments, $q \sim 1$ GeV, around the quasielastic peak. For these kinematics it was seen that the frozen approximation gives results very close to the exact value. The frozen approximation was also found to be quite accurate in the 2p2h MEC

responses [55]. and in the semi-empirical formula of the MEC responses [23].

V. RESULTS

In this section, we extend the superscaling model introduced in Section II and perform a new analysis of the (e, e') data assuming that the scaling function contains a contribution from 2p2h that produces the tail of the quasielastic scaling data. Therefore, in the extended scaling model, we replace the quasielastic superscaling function f_{QE}^* with $f_{1p1h}^* + f_{2p2h}^*$. The 2p2h component of the scaling function is parameterized using the semi-empirical formula for the 2p2h response discussed in the previous section, and thus it is proportional to the phase space function $F(q, \omega)$. This can be seen as an alternative to the traditional superscaling analysis, which typically parametrizes the 2p2h component using Gaussian functions, while in this approach, we impose an additional condition.

The extended scaling analysis is carried out in three steps: i) A preliminary scaling analysis is performed as usual to obtain the function f_{QE}^* , after subtracting the contribution of the MEC from the data, Eq. (17). ii) For each value of q , the 2p2h parameter is adjusted such that the function f_{2p2h}^* reproduces the high-energy tail of the scaling function f_{QE}^* . iii) The contribution of f_{2p2h}^* is subtracted from the data, and a new scaling analysis is performed to extract the 1p1h scaling function f_{1p1h}^* .

After this procedure, it is observed that the resulting f_{1p1h}^* function is compatible with a symmetric function, indicating that the assumed dependence for the tail is appropriate. In other words, the tail of the scaling function is consistent with the phase space function, and this is in agreement with the hypothesis that the tail is generated by 2p2h excitations. This is why the symmetric scaling function is referred to as f_{1p1h}^* because it no longer includes 2p2h contributions, which have been subtracted from the analysis.

For each value of q , the coefficient $c^{pn}(q)$ is fitted from the phenomenological scaling function f_{QE}^* under the hypothesis that the high energy tail ($\psi^* > 1$) is produced mainly by 2p2h excitations, In Fig. 2 we show the experimental data of f_{QE}^* for ^{12}C and for different q -values. These data have been obtained from the inclusive cross section by subtracting the 2p2h MEC contribution and dividing by the single nucleon cross section, Eq. (18). The Fermi momentum is $k_F = 225$ MeV/c and $M^* = m_N^*/m_N = 0.8$ [22]. The errors of these parameters were estimated in ref [41] in a χ^2 fit. They are $\Delta k_F = 8$ MeV/c and $\Delta M^* = 0.044$. From the figure we see that the scaling is only approximate and the data are concentrated in a narrow band. The band is shown in Fig. 3 for $q \leq 1000$ MeV/c. The scaling model is based on two assumptions; first the single-nucleon factorization, which can be done assuming that the FSI are small in the quasielastic region. The second assumes that the scaling

q [GeV/c]	0.1	0.2	0.3	0.4	0.5	0.6	0.7	0.8	0.9	1
$c^{pn}(\alpha = 0)$	8067	2750	1558	1008	733	550	458	367	312	275
$c^{pn}(\alpha = \frac{1}{18})$	7710	2628	1489	964	701	526	438	350	298	263

TABLE I: Coefficients of the semiempirical formula for different values of the parameter α . The estimated error of $c^{pn}(q)$ is 38%.

function depends solely on the scaling variable, which is a consequence of approximating the nuclear system by an infinite Fermi gas. The small scaling violation can be attributed to nuclear effects that breaks this approximation such as FSI, finite size and off-shell effects. Still the band of Fig. 3 is well defined following the shape of an asymmetric bell, with an evident tail on the right. The phenomenological scaling function of the SuSAM* model is obtained by fitting a sum of Gaussians to this band:

$$f_{QE}^*(\psi^*) = a_3 e^{-(\psi^* - a_1)^2 / (2a_2^2)} + b_3 e^{-(\psi^* - b_1)^2 / (2b_2^2)}. \quad (46)$$

Note that there are no QE data above $\psi^* = 1.5$. Then it is not possible to know from the data how the tail would extend above this value. This is because the region $\psi^* > 1.5$ requires high values of the energy far from the QE region. For low q there are not enough cross section data in this region, and for higher momentum transfer, $q > 500$ MeV/c we enter the inelastic zone with pion emission and the data no longer scale.

If we assume that the tail of the scaling function is primarily due to the emission of two nucleons, then the semiempirical formula offers a theoretical framework to extrapolate the model to high values of ψ^* (or high energy transfer ω). This hypothesis is supported by numerous calculations [26, 33, 56, 57] which have shown that 2p2h inclusive responses exhibit an increasing behavior with energy transfer, contributing to the formation of a tail in the cross section at high energies. Although these calculations are based on various MEC and/or SRC models using different approaches, they all qualitatively resemble the 2p2h phase space, which aligns with the semiempirical approach proposed in this work.

In Fig. 2 we show the 2p2h contribution to the scaling function using the semiempirical formula, for different values of $q \leq 2000$ MeV/c. In all panels the SuSAM* scaling function, $f_{QE}^*(\psi^*)$, is also shown. The 2p2h results have been obtained by dividing the semiempirical formula, Eq. (42) by the averaged cross section of the single nucleon as in Eq. (17)

$$f_{2p2h}^* \equiv \frac{(\frac{d\sigma}{d\Omega d\omega})_{2p2h}}{\sigma_M(v_L r_L + v_T r_T)}. \quad (47)$$

Dividing Eq. (42) over (18) this gives

$$f_{2p2h}^*(q, \omega) = \frac{VF(q, \omega) m_N^* \eta_F^3 \kappa Z + \alpha(Z-1) c^{pn}(q)}{(2\pi)^9 Z \xi_F 2Z-1 m_N^2 m_\pi^4}. \quad (48)$$

Note first that $f_{2p2h}^*(q, \omega)$ does not scale, i.e., it depends on ψ but also on q . Second the dependency on energy

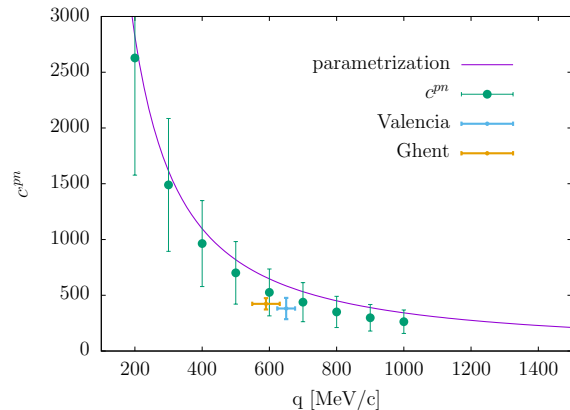


FIG. 4: Fitted values of the coefficients of the semiempirical formula with error bars compared to the interpolating function of Eq. (49).

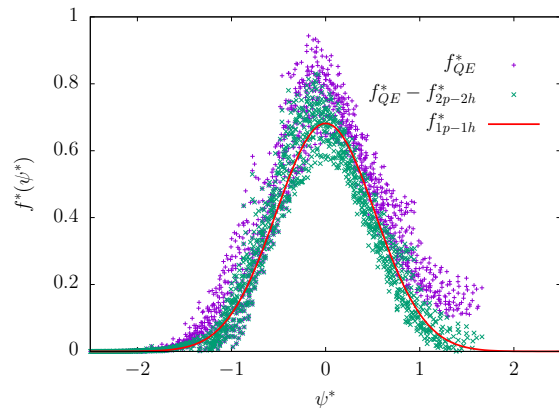


FIG. 5: Experimental values of the scaling function of ^{12}C before and after the subtraction of the 2p2h contribution. The solid line is the new SuSAM* 1p1h scaling function.

of $f_{2p2h}^*(q, \omega)$ comes solely from phase-space. This is because the single nucleon cross section has canceled with the denominator in Eq. (47). Then here the 2p2h contribution to the scaling function is parametrized with a function increasing with energy as the phase space times a parameter that is q -dependent. The 2p2h parameter $c^{pn}(q)$ is chosen to make f_{2p2h}^* to coincide with the tail of the scaling function for $\psi^* = 1.5$. The 2p2h coefficients are given in Table 1 for $q = 100$ up to 1000 MeV/c. In the table we provide two sets of coefficients corresponding to the parameter $\alpha = 1/18$ and also $\alpha = 0$ (neglecting the pp and nn contribution). It is found that the coefficient $c^{pn}(q)$ decreases with q . Roughly it behaves as $c^{pn}(q) \sim 1/q$.

Since the experimental data of the scaling function are distributed in a thick band, as seen in Fig. 2, the coefficients $c^{pn}(q)$ have an uncertainty that can be estimated by fitting the lower or upper part of the band for $\psi^* = 1.5$. The error in $c^{pn}(q)$ is approximately 38% and it is large because it corresponds to the uncertainty of

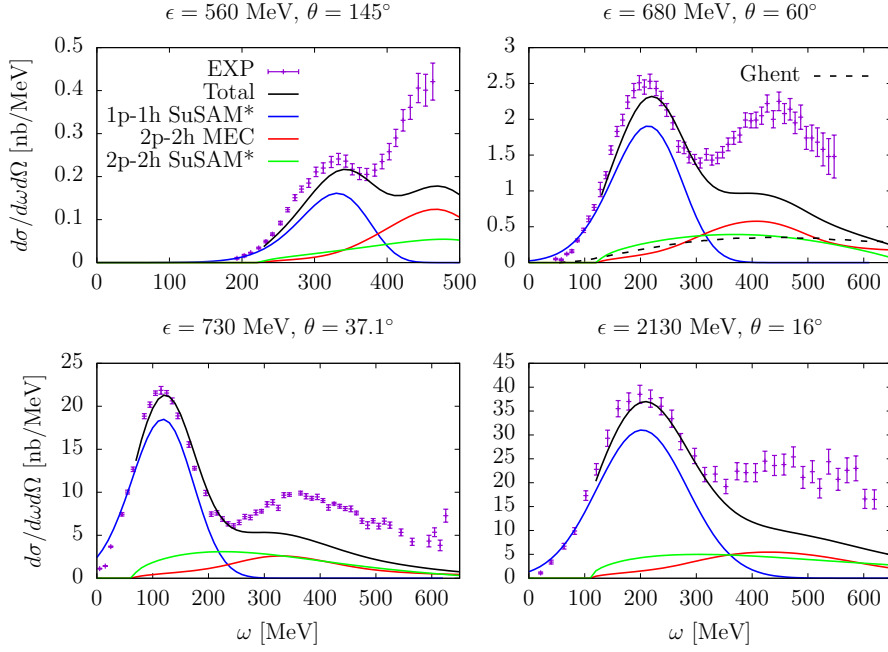


FIG. 6: Calculations of the $^{12}\text{C}(e, e')$ cross section in the separated 1p1h, 2p2h, and MEC channels for several kinematics. The total is the sum of the three channels. In the case $\epsilon = 680$ MeV we compare with the SRC-2p2h of Ref. [26]. The experimental data are from [51, 52].

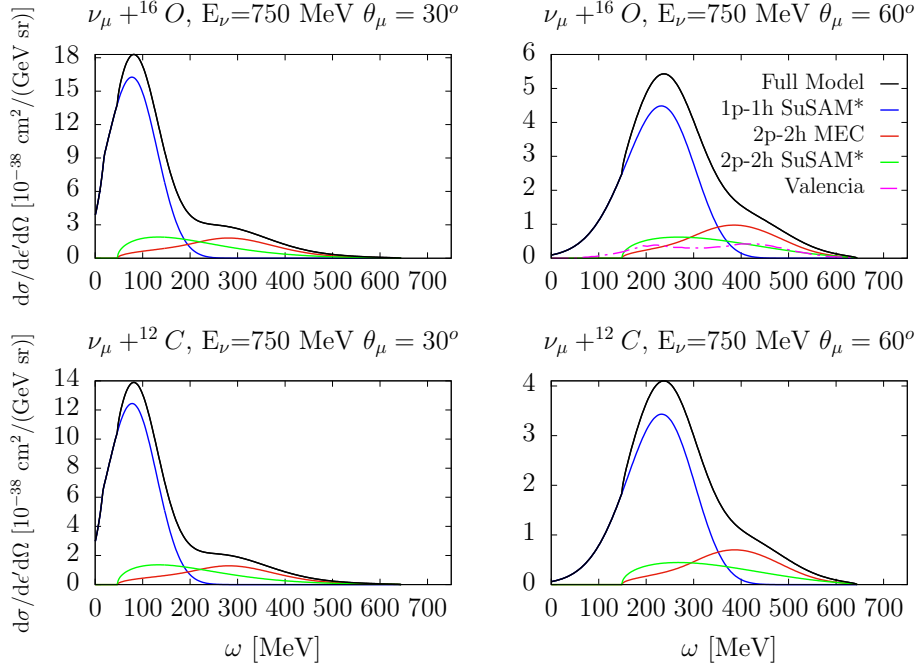


FIG. 7: Calculations of the ^{12}C and $^{16}\text{O}(\nu_\mu, \mu)$ cross section in the separated 1p1h, 2p2h, and MEC channels for fixed neutrino energy. The total is the sum of the three channels. In the case ^{16}O , $\theta_\mu = 60^\circ$ we compare with the 2p2h model of Ref. [13]

the scaling function in the tail zone for $\psi^* = 1.5$.

Our fit has been made for $q \leq 1000$ MeV/c that is the region of interest for electron and neutrino scattering. For higher q the right side of the QE peak is missing from the data due to pion emission. In fig. 3 we show the contribution f_{2p2h}^* calculated with Eq (48) for the kinematics of all the QE experimental data with $q < 1000$

MeV/c. We see that these points generate a band that can explain the tail of the scaling function. To compute f_{2p2h}^* for arbitrary q -values we have interpolated the coefficients $c^{pn}(q)$ using the formula

$$c^{pn}(q) = a_0 \sqrt{\frac{m_N^* + q}{q} \frac{m_N^*}{q}} \quad (49)$$

that fits well the q dependence of $c^{pn}(q)$ with the parameter $a_0 = 345 \pm 130$, for $\alpha = 1/18$ (see Fig. 4).

As an example, the decrease of $c^{pn}(q)$ is also expected in the particular case of the independent-pair factorized model. In fact it can be observed from Eq. (28) that the high-momentum function $\Delta\varphi_{\mathbf{h}_1\mathbf{h}_2}(\mathbf{p})$ has a denominator of $h^2 - p^2$, causing the average distribution $|\Delta\varphi_{\mathbf{h}_1\mathbf{h}_2}(\mathbf{p} + \mathbf{q}/2)|^2$ to rapidly diminish as q increases. However in this simplified model, the precise dependence may not necessarily follow the exact form described by equation (49).

Once the coefficients of the semiempirical formula have been fitted, we propose to carry out a new scaling analysis without the contribution of the emission of two particles. To do this we subtract the f_{2p2h}^* contribution from the f_{QE}^* data. Since the MEC contribution had already been subtracted, the new data no longer contain 2p2h contribution and can thus be considered purely 1p1h data. The result of this new scaling analysis is shown in Fig. 5. As we see, after the subtraction a new band of points is obtained that is symmetrical, since the emission of two nucleons has been eliminated. A new phenomenological scaling function can now be fitted with a Gaussian

$$f_{1p1h}^*(\psi^*) = be^{-(\psi^*)^2/a^2}. \quad (50)$$

The fitted coefficients are $a=0.744\pm 0.082$ and $b = 0.682\pm 0.102$. The errors in the parameters have been estimated by fitting Gaussians to the upper and lower part of the band.

With the present approach we can compute the inclusive effective section of electrons and neutrinos by adding separately the contributions of SuSAM* 1p1h+2p2h plus MEC contributions.

$$\frac{d\sigma}{d\Omega'de'} = \left(\frac{d\sigma}{d\Omega'de'}\right)_{1p1h} + \left(\frac{d\sigma}{d\Omega'de'}\right)_{2p2h} + \left(\frac{d\sigma}{d\Omega'de'}\right)_{MEC}, \quad (51)$$

where the 1p1h cross section is computed with the scaling function (50), the 2p2h with the semiempirical formula fitted above, and the MEC with the semiempirical formula fitted in [23].

Results are shown in Fig. 6 for electrons and Fig. 7 for neutrinos. In Fig. 6 we show the inclusive cross section of ^{12}C for several kinematics as a function of ω . We show the separate contributions of the three terms of Eq. (51) and the total contribution of the model. The pion emission is not included.

The ω -dependence of the SuSAM*-2p2h is similar to the MEC contribution and extends from the QE peak to the dip region and also to the Δ region. The order of magnitude is similar to the MEC, except at the Δ -peak where the MEC are larger. For incident electron energy $\epsilon = 680$ MeV we compare with the SRC model of ref [26] whose results are quite similar to ours. The present results are also similar to the SRC calculation of $^{56}\text{Fe}(e, e')$ of ref. [58].

A similar behavior is seen in Fig. 7 where we show the (ν_μ, μ) cross section from ^{16}O and ^{12}C for fixed neutrino

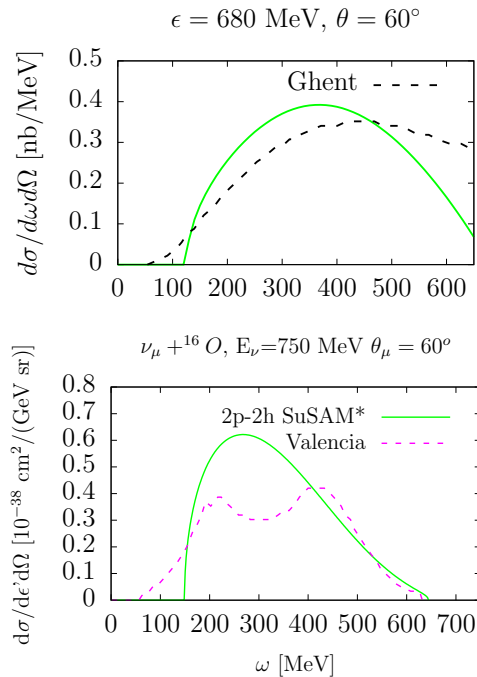


FIG. 8: Detailed comparison of the SuSAM*-2p2h results with the models of refs. [13, 26] for electron and neutrino scattering.

energy and for two scattering angles as a function of ω . A comparison with the SRC results of [13] is also shown for ^{16}O and $\theta_\mu = 60^\circ$.

In Fig. 8, we present a detailed comparison between the SuSAM* 2p2h contribution to the cross section and the SRC models discussed in references [26] and [13]. Firstly, we observe that both models exhibit a similar dependence on ω , which is consistent with the 2p2h phase space upon which our parametrization of the scaling function tail is based. Additionally, the order of magnitude of the cross-section is similar to what is obtained with our parametrization of the 2p2h scaling function. This suggests that both models reasonably describe the tail of the phenomenological scaling function.

This comparison provides further support for the idea that the tail of the scaling function can be attributed to 2p2h contributions and that our parametrization captures its behavior effectively. However, it's important to note that while these models exhibit qualitative agreement, there may still be quantitative differences due to various factors such as different assumptions, formalism, or input parameters used in each model.

Using the results of these models, we can take advantage of them to readjust the coefficient $c^{pn}(q)$ that results from a microscopic calculation. In the case of the Ghent calculation, the kinematics correspond to momentum transfer values varying in a small interval around $q = 600$ MeV/c. The fit to the semiempirical formula of 2p2h provides a theoretical value of the coefficient $c^{pn}(q)$, which is shown as a data point in Figure 4. We see that its value is slightly lower than the SuSAM* value but within its uncertainty interval. The kinematics of the Valencia

model corresponds to q values around 650 MeV/c. The adjusted value of $c^{pn}(q)$ to this model also shown as a data point in Fig. 4, is also below the SuSAM* value from, but always within the error interval.

Using the results of these microscopic models to readjust the 2p2h parameter is a valid approach. While there are differences between the microscopic models and our semiempirical formula, the adjusted values of $c^{pn}(q)$ obtained from these models are consistent with our fits and within the error intervals. Indeed, the comparison between different theoretical calculations, such as those based on electrons and neutrinos and involving different kinematics, can provide valuable insights into the compatibility and consistency of these models. The fact that our phenomenological parameterization of the 2p2h function in the SuSAM* scaling analysis shows agreement with these theoretical calculations highlights another useful aspect of the extended scaling approach.

The parameterization of the 2p2h response presented in this scaling analysis is similar to the pure phase-space model proposed by Mosel et al. [61], which is implemented in the GiBUU event generator. In this scheme, the 2p2h response is parametrized as the product of the 2p2h phase-space and the dipole electromagnetic form factor, which is proportional to the single-nucleon response in our parameterization. The present work further strengthens the validity of this approach for its use in neutrino scattering cross-section calculations. Additionally, the parameters of our model are alternatively fitted to quasielastic scaling data, which is associated with the high-energy tail of the electron scattering data. This highlights the potential of this approach to describe both quasielastic and 2p2h processes in neutrino-nucleus scattering and supports its application in the analysis of neutrino scattering experiments.

VI. CONCLUSIONS

In conclusion, this work presents an extension of the superscaling analysis of electron scattering data using a new parameterization of the phenomenological scaling function in the quasielastic peak. The new parameterization assumes that the high-energy tail of the scaling function is produced by the emission of two nucleons with the one-body (OB) current through the 2p2h phase space function. By incorporating this 2p2h contribution and considering the interference effects with two-body currents and other processes, we account for the phenomenologi-

cal aspects of two-nucleon emission with the OB current and its contributions to scaling violation.

The new parameterization allows for the restoration of symmetry in the 1p1h scaling function with respect to the scaling variable ψ^* . It effectively separates the 1p1h and 2p2h contributions, providing a clearer understanding of the underlying physics in the scaling analysis. Importantly, the new 1p1h+2p2h parameterization describes the experimental data as well as the traditional parameterization. It captures the features of the scaling function, including the tail region, and provides a consistent description of the observed scaling phenomena.

We have also studied a simple model based on the independent-pairs approximation to investigate the basic structure of two-particle emission in the factorized scaling analysis. In this schematic model, the 2p2h parameters are related to the average high-momentum distribution in a 2p2h excitation. In reality, the coefficients that characterize the high-energy tail of the scaling function encompass additional entangled contributions, including interference effects from MEC and FSI. Although the current phenomenological analysis offers valuable initial insights, a comprehensive understanding of the influence of SRCs on the scaling function's high-energy tail necessitates a more detailed investigation using a realistic model.

An important utility of this extended scaling analysis is that it provides a procedure to derive a simplified expression for the two-nucleon emission cross section in nuclei. This simplified expression can be valuable in reducing the computational effort required for simulations of neutrino-nucleus interactions. By parametrizing the 2p2h response, it also offers a method to compare different models of the process, including comparisons between electron scattering and neutrino scattering at different kinematics. This capability can be particularly useful in Monte Carlo event generators used for the analysis of neutrino oscillation experiments with accelerators.

VII. ACKNOWLEDGMENTS

Work supported by: Grant PID2020-114767GB-I00 funded by MCIN/AEI/10.13039/501100011033; FEDER/Junta de Andalucía-Consejería de Transformación Económica, Industria, Conocimiento y Universidades/A-FQM-390-UGR20; and Junta de Andalucía (Grant No. FQM-225).

Appendix A: Matrix element of the OB current with correlated nucleons

Here we derive the matrix element of the OB current between a correlated pair and a two-particle state above the Fermi level, Eqs. (29,30). It is obtained as the sum of the OB current acting on each of the particles.

$$\langle [\mathbf{p}'_1 \mathbf{p}'_2] | J_{OB}^\mu(\mathbf{q}) | [\Phi_{\mathbf{h}_1 \mathbf{h}_2}] \rangle = \langle [\mathbf{p}'_1 \mathbf{p}'_2] | J_1^\mu + J_2^\mu | [\Delta \Phi_{\mathbf{h}_1 \mathbf{h}_2}] \rangle \quad (\text{A1})$$

Let's calculate the matrix element of J_1^μ writing explicitly the spin indices. We assume that the two-hole uncorrelated state is $|\mathbf{h}_1 s_1 \mathbf{h}_2 s_2\rangle$. The corresponding correlated wave function is denoted by

$$|\Phi_{\mathbf{h}_1 \mathbf{h}_2}^{s_1 s_2}\rangle = |\mathbf{h}_1 s_1 \mathbf{h}_2 s_2\rangle + |\Delta\Phi_{\mathbf{h}_1 \mathbf{h}_2}^{s_1 s_2}\rangle \quad (\text{A2})$$

where $|\Delta\Phi_{\mathbf{h}_1 \mathbf{h}_2}^{s_1 s_2}\rangle$ carries the high momentum components. First we introduce a complete set of momentum states

$$\langle[\mathbf{p}'_1 s'_1 \mathbf{p}'_2 s'_2]|J_1^\mu|[\Delta\Phi_{\mathbf{h}_1 \mathbf{h}_2}^{s_1 s_2}]\rangle = \int d^3 p_1 d^3 p_2 \sum_{\sigma_1 \sigma_2} \langle[\mathbf{p}'_1 s'_1 \mathbf{p}'_2 s'_2]|J_1^\mu|\mathbf{p}_1 \sigma_1 \mathbf{p}_2 \sigma_2\rangle \langle\mathbf{p}_1 \sigma_1 \mathbf{p}_2 \sigma_2|[\Delta\Phi_{\mathbf{h}_1 \mathbf{h}_2}^{s_1 s_2}]\rangle \quad (\text{A3})$$

The first matrix element inside the integral is

$$\begin{aligned} \langle[\mathbf{p}'_1 s'_1 \mathbf{p}'_2 s'_2]|J_1^\mu|\mathbf{p}_1 \sigma_1 \mathbf{p}_2 \sigma_2\rangle &= \langle[\mathbf{p}'_1 s'_1]|J_1^\mu|[\mathbf{p}_1 \sigma_1]\rangle \langle\mathbf{p}'_2 s'_2|\mathbf{p}_2 \sigma_2\rangle \\ &= \frac{(2\pi)^3}{V} \delta(\mathbf{p}'_1 - \mathbf{p}_1 - \mathbf{q}) j_{OB}^\mu(\mathbf{p}'_1, \mathbf{p}'_1 - \mathbf{q})_{s'_1 \sigma_1} \delta(\mathbf{p}'_2 - \mathbf{p}_2) \delta_{s'_2 \sigma_2} \end{aligned} \quad (\text{A4})$$

where j_{OB} is the OB current function given in Eq. (8) in the electromagnetic case, and we have exchanged the bracket of \mathbf{p}'_2 for \mathbf{p}_1 . The matrix element of the high-momentum wave function is

$$\begin{aligned} \langle\mathbf{p}_1 \sigma_1 \mathbf{p}_2 \sigma_2|[\Delta\Phi_{\mathbf{h}_1 \mathbf{h}_2}^{s_1 s_2}]\rangle &= \frac{(2\pi)^3}{V} \langle\mathbf{p}_1 \sigma_1 \mathbf{p}_2 \sigma_2|\Delta\Phi_{\mathbf{h}_1 \mathbf{h}_2}^{s_1 s_2}\rangle \\ &= \frac{(2\pi)^3}{V} \delta(\mathbf{p}'_1 + \mathbf{p}'_2 - \mathbf{h}_1 - \mathbf{h}_2) \Delta\varphi_{\mathbf{h}_1 \mathbf{h}_2}^{s_1 s_2}(\mathbf{p})_{\sigma_1 \sigma_2} \end{aligned} \quad (\text{A5})$$

Inserting Eqs. (A4,A5) in (A3) and integrating using the Dirac deltas we obtain

$$\langle[\mathbf{p}'_1 s'_1 \mathbf{p}'_2 s'_2]|J_1^\mu|[\Delta\Phi_{\mathbf{h}_1 \mathbf{h}_2}^{s_1 s_2}]\rangle = \frac{(2\pi)^6}{V^2} \delta(\mathbf{p}'_1 + \mathbf{p}'_2 - \mathbf{q} - \mathbf{h}_1 - \mathbf{h}_2) \sum_{\sigma_1} j_{OB}^\mu(\mathbf{p}'_1, \mathbf{p}'_1 - \mathbf{q})_{s'_1 \sigma_1} \Delta\varphi_{\mathbf{h}_1 \mathbf{h}_2}^{s_1 s_2} \left(\frac{\mathbf{p}'_1 - \mathbf{p}'_2 - \mathbf{q}}{2} \right)_{\sigma_1 s'_2}. \quad (\text{A6})$$

Proceeding analogously to calculate the matrix element of J_2 , we obtain the equation

$$\langle[\mathbf{p}'_1 s'_1 \mathbf{p}'_2 s'_2]|J_2^\mu|[\Delta\Phi_{\mathbf{h}_1 \mathbf{h}_2}^{s_1 s_2}]\rangle = \frac{(2\pi)^6}{V^2} \delta(\mathbf{p}'_1 + \mathbf{p}'_2 - \mathbf{q} - \mathbf{h}_1 - \mathbf{h}_2) \sum_{\sigma_2} j_{OB}^\mu(\mathbf{p}'_2, \mathbf{p}'_2 - \mathbf{q})_{s'_2 \sigma_2} \Delta\varphi_{\mathbf{h}_1 \mathbf{h}_2}^{s_1 s_2} \left(\frac{\mathbf{p}'_1 - \mathbf{p}'_2 + \mathbf{q}}{2} \right)_{s'_1 \sigma_2}. \quad (\text{A7})$$

By analogy with Equation (21), the 2p2h correlation current function turns out to be

$$\begin{aligned} j_{cor}(\mathbf{p}'_1, \mathbf{p}'_2, \mathbf{h}_1, \mathbf{h}_2) &= (2\pi)^3 \sum_{\sigma} j_{OB}^\mu(\mathbf{p}'_1, \mathbf{p}'_1 - \mathbf{q})_{s'_1 \sigma} \Delta\varphi_{\mathbf{h}_1 \mathbf{h}_2}^{s_1 s_2} \left(\frac{\mathbf{p}'_1 - \mathbf{p}'_2 - \mathbf{q}}{2} \right)_{\sigma s'_2} \\ &\quad + (2\pi)^3 \sum_{\sigma} j_{OB}^\mu(\mathbf{p}'_2, \mathbf{p}'_2 - \mathbf{q})_{s'_2 \sigma} \Delta\varphi_{\mathbf{h}_1 \mathbf{h}_2}^{s_1 s_2} \left(\frac{\mathbf{p}'_1 - \mathbf{p}'_2 + \mathbf{q}}{2} \right)_{s'_1 \sigma}. \end{aligned} \quad (\text{A8})$$

Appendix B: Averaged single-nucleon responses in the SuSAM* model

The single-nucleon responses can be extended beyond values $|\psi^*| > 1$ using the energy distribution function (B1) obtained from the superscaling function by differentiating the two sides of the equation (14) with respect to ϵ_0

$$n(\epsilon_0) = -\frac{2}{3} \frac{1}{\psi^*} \frac{df^*(\psi^*)}{d\psi^*}. \quad (\text{B1})$$

We use the non-correlated superscaling function $f^*(\psi^*) = b \exp(-(\psi^*)^2/a^2)$ to compute the energy distribution and the averaged single-nucleon responses, Eq.

(12), giving $n(\epsilon_0) = -\frac{4}{3a^2} f^*(\psi^*)$. The single-nucleon responses $U_K(\epsilon, q, \omega)$ for neutrinos (antineutrinos) are given in the Appendix C of Ref. [2]. The averaged single-nucleon responses after integration over ϵ are given by

$$\begin{aligned} \bar{U}_{CC} &= -w_1 \frac{\kappa^2}{\tau} + w_2 \lambda^2 + 2\lambda w_2 [1 + \xi_F(\psi^{*2} + a^2)] \\ &\quad + w_2 [1 + 2\xi_F(\psi^{*2} + a^2) + \xi_F^2(\psi^{*4} + 2a^2\psi^{*2} + 2a^4)] \\ &\quad + 4\lambda^2 w_4, \end{aligned} \quad (\text{B2})$$

$$\begin{aligned} \overline{U}_{CL} = & \frac{\lambda}{\kappa} \left\{ w_1 \frac{\kappa^2}{\tau} - w_2 \lambda^2 - 2\lambda w_2 [1 + \xi_F(\psi^{*2} + a^2)] \right. \\ & \left. - w_2 [1 + 2\xi_F(\psi^{*2} + a^2) + \xi_F^2(\psi^{*4} + 2a^2\psi^{*2} + 2a^4)] \right\} \\ & - 4\lambda\kappa w_4, \end{aligned} \quad (\text{B3})$$

$$\begin{aligned} \overline{U}_{LL} = & \frac{\lambda^2}{\kappa^2} \left\{ -w_1 \frac{\kappa^2}{\tau} + w_2 \lambda^2 + 2\lambda w_2 [1 + \xi_F(\psi^{*2} + a^2)] \right. \\ & \left. + w_2 [1 + 2\xi_F(\psi^{*2} + a^2) + \xi_F^2(\psi^{*4} + 2a^2\psi^{*2} + 2a^4)] \right\} \\ & + 4\kappa^2 w_4, \end{aligned} \quad (\text{B4})$$

$$\begin{aligned} \overline{U}_T = & 2w_1 + 2w_2 \lambda \frac{\tau}{\kappa^2} [1 + \xi_F(\psi^{*2} + a^2)] - w_2 \\ & + w_2 \frac{\tau}{\kappa^2} [1 + 2\xi_F(\psi^{*2} + a^2) + \xi_F^2(\psi^{*4} + 2a^2\psi^{*2} + 2a^4)] \\ & - \frac{\tau^2}{\kappa^2} w_2, \end{aligned} \quad (\text{B5})$$

$$\overline{U}_{T'} = 2w_3 \frac{\tau}{\kappa} \left\{ \lambda + [1 + \xi_F(\psi^{*2} + a^2)] \right\}. \quad (\text{B6})$$

The single-nucleon structure functions, w_1 , w_2 , w_3 and w_4 are given [2] by

$$w_1 = \tau(2G_M^{*V})^2 + (1 + \tau)G_A^2, \quad (\text{B7})$$

$$w_2 = \frac{(2G_E^{*V})^2 + \tau(2G_M^{*V})^2}{1 + \tau} + G_A^2, \quad (\text{B8})$$

$$w_3 = G_A 2G_M^{*V}, \quad (\text{B9})$$

$$w_4 = \frac{(G_A - \tau G_P^*)^2}{4\tau}, \quad (\text{B10})$$

where G_E^{*V} and G_M^{*V} are the electric and magnetic isovector form factors $G_{E,M}^{*V} = (G_{E,M}^{*P} - G_{E,M}^{*N})/2$ modified in the medium with the relativistic effective mass [59]. For the axial form factor, G_A , we use dipole parametrization with axial mass $M_A = 1.032$ GeV. Finally the pseudoscalar form factor $G_P^* = 4m_N m_N^* G_A / (m_\pi^2 - Q^2)$.

For electron scattering the equations are similar for $\overline{U}_L = \overline{U}_{CC}$ and \overline{U}_T , without the axial contribution, $w_3 = w_4 = 0$. For protons and neutrons the corresponding structure functions are

$$w_1^{em} = \tau(G_M^*)^2, \quad (\text{B11})$$

$$w_2^{em} = \frac{(G_E^*)^2 + \tau(G_M^*)^2}{1 + \tau}, \quad (\text{B12})$$

with the electric and magnetic form factors

$$G_E^* = F_1 - \tau \frac{m_N^*}{m_N} F_2, \quad G_M^* = F_1 + \frac{m_N^*}{m_N} F_2. \quad (\text{B13})$$

For the F_i form factors of the nucleon, we use the Galster parameterization [60].

-
- [1] A. M. Ankowski, A. Ashkenazi, S. Bacca, J. L. Barrow, M. Betancourt, A. Bodek, M. E. Christy, L. D. S. Dytman, A. Friedland and O. Hen, *et al.* [arXiv:2203.06853 [hep-ex]].
- [2] J. E. Amaro, M. B. Barbaro, J. A. Caballero, R. González-Jiménez, G. D. Megias and I. Ruiz Simo, *J. Phys. G* **47** (2020) no.12, 124001
- [3] U. Mosel, *Ann. Rev. Nuc. Part. Sci.* **66** (2016), 171.
- [4] T. Katori and M. Martini, *J. Phys. G* **45** (2018) no.1, 013001.
- [5] L. Alvarez-Ruso, Y. Hayato, J. Nieves, *New J. Phys.* **16** (2014) 075015.
- [6] A. M. Ankowski, C. Mariani, *J. Phys. G* **44** (2017) 054001.
- [7] O. Benhar, P. Huber, C. Mariani, D. Meloni, *Phys. Rep.* **700** (2017) 1.
- [8] R. Rosenfelder, *Ann. Phys. (N.Y.)* **128**, 188 (1980).
- [9] B.D. Serot, and J.D. Walecka, *Adv. Nucl. Phys.* **16** (1986) 1.
- [10] D Drechsel and M M Giannini, *Rep. Prog. Phys.* **52** (1989) 1083.
- [11] K. Wehrberger, *Phys. Rep.* **225** (1993) 273.
- [12] M. Martini, M. Ericson, G. Chanfray, J. Marteau, *Phys.Rev. C* **80** (2009) 065501.
- [13] J. Nieves, I. Ruiz Simo, M.J. Vicente Vacas, *Phys.Rev. C* **83** (2011) 045501.
- [14] K. Gallmeister, U. Mosel and J. Weil, *Phys. Rev. C* **94**, no. 3, 035502 (2016).
- [15] G. D. Megias, M. V. Ivanov, R. Gonzalez-Jimenez, M. B. Barbaro, J. A. Caballero, T. W. Donnelly and J. M. Udias, *Phys. Rev. D* **89**, no. 9, 093002 (2014) Erratum: [*Phys. Rev. D* **91**, no. 3, 039903 (2015)]
- [16] G.D Megias, J. E. Amaro, M. B. Barbaro, J. A. Caballero, T. W. Donnelly and I. Ruiz Simo, *Phys. Rev. D* **94** (2016), 093004.
- [17] G. D. Megias, J. E. Amaro, M. B. Barbaro, J. A. Caballero and T. W. Donnelly, *Phys. Rev. D* **94**, 013012 (2016).
- [18] A. M. Ankowski, *Phys. Rev. D* **92**, no. 1, 013007 (2015).
- [19] R. Gran, J. Nieves, F. Sanchez and M. J. Vicente Vacas, *Phys. Rev. D* **88**, no. 11, 113007 (2013).
- [20] V. Pandey, N. Jachowicz, M. Martini, R. Gonzalez-Jimenez, J. Ryckebusch, T. Van Cuyck and N. Van Dessel, *Phys. Rev. C* **94**, no. 5, 054609 (2016)
- [21] M. Martini, N. Jachowicz, M. Ericson, V. Pandey, T. Van Cuyck and N. Van Dessel, *Phys. Rev. C* **94**, no. 1, 015501 (2016).

- [22] V. L. Martinez-Consentino, I. R. Simo and J. E. Amaro, Phys. Rev. C **104**, no.2, 025501 (2021)
- [23] V. L. Martinez-Consentino, J. E. Amaro and I. Ruiz Simo, Phys. Rev. D **104**, no.11, 113006 (2021)
- [24] A. De Pace, M. Nardi, W. M. Alberico, T. W. Donnelly and A. Molinari, Nucl. Phys. A **726**, 303-326 (2003)
- [25] I. Ruiz Simo, J. E. Amaro, M. B. Barbaro, A. De Pace, J. A. Caballero and T. W. Donnelly, J. Phys. G **44**, no.6, 065105 (2017)
- [26] T. Van Cuyck, N. Jachowicz, R. González-Jiménez, M. Martini, V. Pandey, J. Ryckebusch and N. Van Dessel, Phys. Rev. C **94**, no.2, 024611 (2016)
- [27] J. Ryckebusch, V. Van der Sluys, K. Heyde, H. Holvoet, W. Van Nespén, M. Waroquier and M. Vanderhaeghen, Nucl. Phys. A **624**, 581-622 (1997)
- [28] S. Stevens, J. Ryckebusch, W. Cosyn and A. Waets, Phys. Lett. B **777**, 374-380 (2018)
- [29] W. Cosyn and J. Ryckebusch, Phys. Lett. B **820**, 136526 (2021)
- [30] W. Alberico, M. Ericson, and A. Molinari, Ann. Phys. (N.Y.) **154** (1984) 356.
- [31] W. M. Alberico, T. W. Donnelly and A. Molinari, Nucl. Phys. A **512**, 541-590 (1990)
- [32] J. E. Amaro, M. B. Barbaro, J. A. Caballero, T. W. Donnelly and A. Molinari, Phys. Rept. **368**, 317-407 (2002)
- [33] J. E. Amaro, C. Maieron, M. B. Barbaro, J. A. Caballero and T. W. Donnelly, Phys. Rev. C **82**, 044601 (2010)
- [34] J. Ryckebusch, W. Cosyn, S. Stevens, C. Casert and J. Nys, Phys. Lett. B **792**, 21-28 (2019)
- [35] I. Ruiz Simo, R. Navarro Pérez, J. E. Amaro and E. Ruiz Arriola, Phys. Rev. C **96**, no.5, 054006 (2017)
- [36] C. Colle, O. Hen, W. Cosyn, I. Korover, E. Piassetzky, J. Ryckebusch and L. B. Weinstein, Phys. Rev. C **92**, no.2, 024604 (2015)
- [37] R. Weiss, A. W. Denniston, J. R. Pybus, O. Hen, E. Piassetzky, A. Schmidt, L. B. Weinstein and N. Barnea, Phys. Rev. C **103**, no.3, L031301 (2021)
- [38] D. Nguyen *et al.* [Jefferson Lab Hall A], Phys. Rev. C **102**, no.6, 064004 (2020)
- [39] J. E. Amaro, I. Ruiz Simo, and E. Ruiz Arriola, Phys. Rev. D **95**, 076009 (2017).
- [40] V. L. Martinez-Consentino, I. Ruiz Simo, J. E. Amaro and E. Ruiz Arriola, Phys. Rev. C **96**, no. 6, 064612 (2017).
- [41] J. E. Amaro, V. L. Martinez-Consentino, E. Ruiz Arriola and I. Ruiz Simo, Phys. Rev. C **98** (2018) 024627
- [42] I. Ruiz Simo, V. L. Martinez-Consentino, J. E. Amaro and E. Ruiz Arriola, Phys. Rev. D **97**, 116006 (2018). MDPI and ACS Style
- [43] P.R. Casale, J.E. Amaro, V.L. Martinez-Consentino, I. Ruiz Simo, Universe **9** (2023) 158.
- [44] A. M. Saruis, Phys. Rept. **235**, 57-188 (1993)
- [45] G. B. West, Phys. Rept. **18**, 263-323 (1975)
- [46] J.D. Walecka, Theoretical Nuclear and Subnuclear Physics, Oxford University Press (New York) 1995.
- [47] I. Ruiz Simo, R. Navarro Pérez, J. E. Amaro and E. Ruiz Arriola, Phys. Rev. C **96**, no.5, 054006 (2017)
- [48] R. Navarro Pérez, J. E. Amaro and E. Ruiz Arriola, Phys. Rev. C **88**, no.6, 064002 (2013) [erratum: Phys. Rev. C **91**, no.2, 029901 (2015)]
- [49] R. Shneor *et al.* [Jefferson Lab Hall A], Phys. Rev. Lett. **99**, 072501 (2007)
- [50] R. Subedi, R. Shneor, P. Monaghan, B. D. Anderson, K. Aniol, J. Annand, J. Arrington, H. Benaoum, W. Bertozzi and F. Benmokhtar, *et al.* Science **320**, 1476-1478 (2008)
- [51] O. Benhar, D. Day and I. Sick, arXiv:nucl-ex/0603032.
- [52] O. Benhar, D. Day, and I. Sick, <http://faculty.virginia.edu/qes-archive/>
- [53] I. Ruiz Simo, C. Albertus, J. E. Amaro, M. B. Barbaro, J. A. Caballero and T. W. Donnelly, Phys. Rev. D **90**, no.5, 053010 (2014)
- [54] I. Ruiz Simo, C. Albertus, J. E. Amaro, M. B. Barbaro, J. A. Caballero and T. W. Donnelly, Phys. Rev. D **90**, no.3, 033012 (2014)
- [55] I. Ruiz Simo, J. E. Amaro, M. B. Barbaro, J. A. Caballero, G. D. Megias and T. W. Donnelly, Phys. Lett. B **770**, 193-199 (2017)
- [56] G. Co' and A. M. Lallena, Annals Phys. **287**, 101-150 (2001)
- [57] G. Co' and A. M. Lallena, Phys. Rev. C **57**, 145-149 (1998)
- [58] Q. Niu, J. Liu, Y. Guo, C. Xu, M. Lyu, and Z. Ren, PhysRev C **105** (2022) L051602.
- [59] J. E. Amaro, E. Ruiz Arriola and I. Ruiz Simo, Phys. Rev. C **92**, no. 5, 054607 (2015).
- [60] S. Galster, H. Klein, J. Moritz, K. H. Schmidt, D. Wegener and J. Bleckwenn, Nucl. Phys. B **32**, 221 (1971).
- [61] U. Mosel, O. Lalakulich and K. Gallmeister, Phys. Rev. D **89**, no.9, 093003 (2014)